A New Molecular Ordering in Helical Liquid Crystals

J. W. Goodby,* M. A. Waugh,‡ S. M. Stein,‡ E. Chin,‡ R. Pindak,‡ and J. S. Patel§

Contribution from the School of Chemistry, The University, Hull, HU6 7RX, England, AT&T Bell Laboratories, Murray Hill, New Jersey 07974, and Bell Communications Research, Redbank, New Jersey 07001. *Received March 6, 1989*

Abstract: In the pursuit of new ferroelectric liquid crystals, a novel intermediary state of matter, the helical smectic A* mesophase, was discovered. This layered phase was found between the isotropic liquid and the smectic C* phase in a variety of optically active (*R*)- and (*S*)-1-methylheptyl 4′-[[(4″-*n*-alkoxyphenyl)propioloyl]oxy]biphenyl-4-carboxylates. In these materials, the temperature at which the transition to the ferroelectric smectic C* phase occurs is relatively close to that of the clearing point. Moreover, the materials show a high degree of chirality. These two properties ensure that the A* phase possesses relatively large molecular fluctuations, which give rise to twist and bend distortions resulting in the stabilization of a helical structure. This new phase is apparently miscible with the classical smectic A phase, thereby classifying it as the chiral modification of the A phase.

Since the discovery of the first liquid-crystalline material in 1888,[1,2] chirality and optical activity have proven to be two of the most fascinating topics of research in orientationally ordered fluids. The cholesteric mesophase, which was the first liquid crystal to be found, exhibits *form optical activity* due to a helical arrangement of its constituent molecules. The helicity of this structure was shown to be dependent on molecular chirality.[3] Recently other phases, such as the blue phases,[4,5] which have a double-twist structure, and the chiral smectic C* phase, which was shown to be the first ferroelectric liquid crystal,[6,7] were characterized and also shown to have helical arrangements of their constituent molecules. On the centenary of the discovery of the first liquid crystal, we report the unearthing of a new intermediary, chiral state of matter; the *helical smectic A* phase.*

In the cholesteric mesophase the molecules are oriented so that their long axes are, on average, parallel to one another. In a preferred direction normal to the long axes of the molecules, there is a macroscopic twist associated with the orientational ordering of the molecules, thereby producing a helical structure. Consequently, the phase has *spiraling orientational order.* In contrast, the smectic C* phase has a local ordering where the molecules are randomly packed in layers with their long axes tilted with respect to the layer planes. On passing from one layer to the next, there is a precession of the tilt direction about an axis normal to the layer planes, thereby forming a helix.[8] In this case the phase has *spiraling tilt orientational ordering* of its molecules. In the newly discovered A* phase the molecules are arranged in layers as in the smectic C* phase, but with their long axes on average normal to the layer planes, as in the smectic A phase. This discounts the possibility of a helix forming normal to the layers. Instead, the helical arrangement of the molecules was found, for the first time, to propagate in a direction parallel to the layer planes, as shown in Figure 1. Therefore, unlike the other helical phases, this phase has a *spiraling layer order.*

In the following sections we report a variety of experiments that led us to delineate this new mesophase and to define some of its physical properties.

Experimental Section

The novel smectic A* phase was discovered in a newly synthesized family of ferroelectric materials, the (*R*)- and (*S*)-1-methylheptyl 4′-[[(4″-*n*-alkoxyphenyl)propioloyl]oxy]biphenyl-4-carboxylates (*n*P1M7).[9] These materials were prepared by the esterification of a number of (4-*n*-alkoxyphenyl)propiolic acids with (*R*)- and (*S*)-1-methylheptyl 4′-hydroxybiphenyl-4-carboxylate. The propiolic acids were synthesized from a variety of 4-*n*-alkoxybenzaldehydes via the preparation of the corresponding dibromostyrenes by the method of Corey and Fuchs.[10] The hydroxybiphenyl-4-carboxylate was prepared by a recently reported adaption of the method of Fischer and Fischer.[11] The final ester products were determined to be pure by reverse-phase high-performance, liquid chromatography, using a Beckman 334 solvent delivery system in conjunction with a 421 controller and 164 variable wavelength UV/visible detector. The chromatographic separations were carried out over octadecylsiloxane (Du Pont Zorbax ODS, 5-μm pore size, 25 × 0.46 cm), with hexane as the eluant. The structures of the final products were determined by a combination of IR, NMR, and MS spectral analysis; the results for each compound were found to be consistent with the predicted structures of the target materials.

Transition temperatures and initial phase assignments were determined for the propiolic esters by thermal optical microscopy using a Zeiss Universal Polarizing light microscope equipped with a Mettler FP52 microfurnace used in conjunction with a FP5 control unit.

Alignment and polarization studies were both carried out in similar experiments where the subject material was confined to a cell constructed from electrically conducting (ITO-coated) glass, which had been previously treated with a surfactant, polybutylene-1,4-terephthalate.[12] The internal surfaces of the cell were unidirectionally buffed in order to give sites for planar, homogeneous growth of the liquid crystal via cooling of the liquid.[13] The distance between the glass plates of each cell was controlled by spacers. Electrical contacts were made directly to the internal surfaces of the glass so that the polarization and aligning properties of the material could be studied in an applied electric field in the usual manner.[14]

Temperatures and heats of transition were determined by differential scanning calorimetry using a Perkin-Elmer DSC 4 calorimeter in conjunction with a thermal analysis data station (TADS). As a check on instrumental accuracy an indium standard was run at 0.5 °C min^{-1}. The measured latent heat, 6.795 cal g^{-1}, compared well with that normally found for indium (6.8 cal g^{-1}). The onset temperature (156.56 °C) was found to be close to the known melting point for indium (156.6 °C).[15]

Structural evidence for distinguishing the smectic A* phase from a cholesteric phase was gained by X-ray diffraction measurements using an 18 kW rotating anode based spectrometer. For thist study unaligned samples of the (*R*)-*n*-dodecyloxy, (*R*)-*n*-tetradecyloxy, and (*R*)-*n*-hexadecyloxy (*n* = 12, 14, 16) enantiomers were prepared in 1-mm glass capillaries. A vertically bent pyrolytic graphite (002) crystal was used to focus Cu Kα X-rays to a 0.5 × 2.0 mm^2 spot on the sample. The

* Present address: The University, Hull. Work done while at AT&T Bell Laboratories, Murray Hill, NJ, 07974.
‡ AT&T Bell Laboratories.
§ Bell Communications Research.

(1) Reinitzer, F. *Monatsh. Chem.* **1888**, *9*, 421.
(2) Lehmann, O. *Z. Phys. Chem. (Leipzig)* **1889**, *4*, 462.
(3) Gray, G. W.; McDonnell, D. G. *Mol. Cryst. Liq. Cryst. Lett.* **1977**, *34*, 211.
(4) Coates, D.; Gray, G. W. *Phys. Lett.* **1973**, *45A*, 115.
(5) Berreman, D. W. *Liquid Crystals and Ordered Fluids*; Griffin, A. C., Johnson, J. F., Eds.; Plenum Press: New York, 1984; Vol. 4, p 925.
(6) Meyer, R. B. *Mol. Cryst. Liq. Cryst.* **1977**, *40*, 33.
(7) Meyer, R. B.; Liebert, L.; Strzelecki, L.; Keller, P. *J. Phys. Lett.* **1976**, *36*, 69.
(8) Doucet, J.; Keller, P.; Levelut, A-M.; Porquet, P. *J. Phys. (Les Ulis, Fr.)* **1978**, *39*, 548.
(9) Waugh, M. A.; Stein, S. M., to be published.
(10) Corey, E. J.; Fuchs, P. L. *Tetrahedron Lett.* **1976**, 3769.
(11) Chin, E.; Goodby, J. W. *Mol. Cryst. Liq. Cryst.* **1986**, *141*, 311.
(12) Patel, J. S.; Leslie, T. M.; Goodby, J. W. *Ferroelectrics* **1984**, *59*, 137.
(13) Patel, J. S.; Goodby, J. W. *J. Appl. Phys.* **1986**, *59*, 2355.
(14) Patel, J. S.; Goodby, J. W. *Chem. Phys. Lett.* **1987**, *137*, 91.
(15) *CRC Handbook of Chemistry and Physics*, 68th ed., Weast, R. C., Ed.; CRC Press: Boca Raton, FL, 1987; p B219.

0002-7863/89/1511-8119$01.50/0

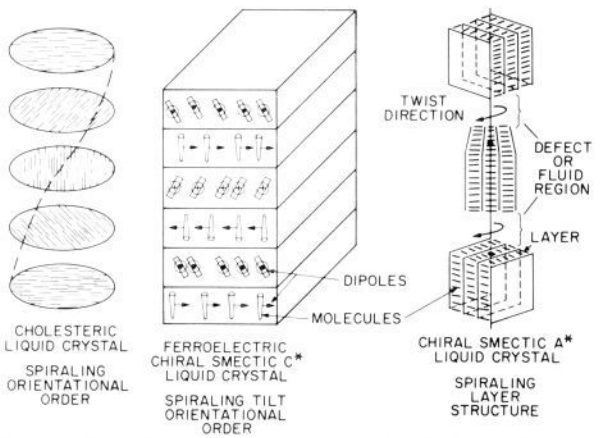

Figure 1. Pictorial representation of some helical liquid-crystal phases, including the cholesteric, the chiral smectic C*, and the chiral smectic A* modifications.

scattered radiation was then analyzed by using slits and a flat pyrolytic graphite crystal. This defined an instrumental resolution of 0.01 $Å^{-1}$ full width at half-maximum in the scan direction, and 0.02-$Å^{-1}$ transverse to the scattering plane.

Results

Liquid Crystals Properties. The phase behavior of the homologous series (*n*P1M7) was studied by a variety of different techniques. At long *n*-alkoxy chain lengths the series was found to contain a novel variation of mesophase behavior in the form of a new liquid-crystal phase, smectic A*. Specifically, the helical A* phase was observed in the *n*-tridecyloxy, the *n*-tetradecyloxy, and the *n*-pentadecyloxy homologues (n = 13, 14, 15), and as a possibility for the *n*-dodecyloxy (n = 12) member of the series. The isotropic liquid to A, A*, or C*, and the A or A* to C* or C transition temperatures for the optically active enantiomers of the series are given in Table I.

Initial studies show that some of the materials also appear to exhibit two further mesophases (S3 and S4). The transitions to and from these "phases" can be detected optically, but not by calorimetry. Consequently, the temperatures, determined by thermal optical microscopy, for these apparent phase transitions are also given in Table I. The properties of the two phases, S3 and S4, were found to be similar in nature to those reported recently for the (*S*)- or (*R*)-1-methylalkyl [[4-(*n*-alkanoyloxy)-benzoyl]oxy]biphenyl-4′-carboxylates.[16] In a way similar to these compounds, the S3 and S4 phases could be either two hitherto unclassified helical smectic modifications, or else they may be related to twist inversions of the helix with respect to temperature. However, in the light of the discovery of the helical A* phase, an alternative speculation is that these two phases may also be related to twist-layer deformations, but in the C* phase this time.

From Table I, it can be seen that the *n*-octyloxy and *n*-nonyloxy members of the series do not show C* phases and only exhibit smectic A phases. At the *n*-decyloxy homologue the smectic C* phase is injected into the series. The A to C* transition temperatures rise as the series is ascended until a direct isotropic liquid to smectic C* transition is detected for the *n*-hexadecyloxy compound. For the proceding three compounds, the *n*-tri-, *n*-tetra, and *n*-pentadecyloxy homologues, the temperature range of the A* phase falls as the A* to C* transition temperatures rise.

Optical Studies. The shorter homologues of the series showed typical textures for the smectic A phase and the smectic C* phase.[17] On cooling, the smectic A phase separated from the isotropic liquid in the form of bâtonnets.[18] These either coalesced to give a focal–conic defect structure or else adhered to the surface to give a homeotropic texture. Subsequent cooling in some cases

(16) Goodby, J. W.; Chin, E. *Liq. Cryst.* **1988**, *3*, 1245.
(17) Friedel, G. *Ann. Phys.* (*Paris*) **1922**, *18*, 273.
(18) Hartshorne, N. H.; Stuart, A. *Crystals and the Polarising Microscope*; Arnold: London, England, 1970; p 521.

Table I. Transition Temperatures Determined[a] for

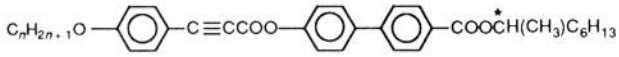

n[b]	iso–A/A*	iso–C*	A/A*–C*[c,e]	C*–S3[d,e,f]	S3–S4[d,e]	mp[g]	recryst[h]
8	97.5					81.3	58.5
ΔH	1.6					11.3	
9	97.5					81.3	58.4
ΔH	1.4					12.1	
10	98.0		[76.3]			85.4	76.8
ΔH	1.5					12.3	
11	95.0		[78.1]	[56.0]	[44.6]	85.1	75.9
ΔH	0.8					12.8	
12	96.3		86.0	[57.3]	[48.0]	82.4	36.4
ΔH	0.9					11.4	
13[i]	94.1		88.3	[57.1]	[43.7]	81.6	33.7
ΔH	0.5					10.8	
14[i]	93.8		89.7	[53.4]	[42.5]	78.3	37.2
ΔH	0.3					11.0	
15[i]	91.6		90.6	(50.0)		76.5	52.0
ΔH	0.2					11.4	
16		99.0				73.4	25.6
ΔH		0.4				10.5	

[a] Temperatures (°C) determined on heating cycles by DSC, or by thermal optical microscopy. [b] ΔH enthalpies of transition in cal g^{-1}. [c] Enthalpies for the A–C* transition were too small to be evaluated. [d] Enthalpies for the C*–S3 and S3–S4 transitions could not be detected by DSC; the results presented were determined by optical microscopy. [e] Values in brackets, monotropic phase transitions. [f] Values in parentheses, transition temperature determined by supercooling. [g] mp, melting point of crystal to smectic A (n = 8–11), crystal to smectic C* (n = 12–16). [h] recryst, recrystallization temperature. [i] Compounds that clearly exhibit a helical A* phase.

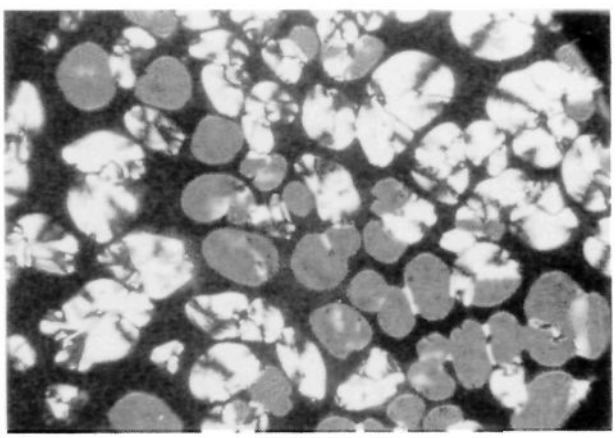

Figure 2. Smectic A* phase separating from the isotropic liquid.

produced a further transition to the smectic C* phase. This phase exhibited paramorphotic defect textures of the A phase. The focal–conic defects became crossed with parallel lines and the pseudohomeotropic texture showed selective reflectance properties, both of which are associated with the helical nature of the phase. The paramorphosis and defect structures of both of these phases were found to be typical, thereby allowing a provisional classification of the phases as A and C*.

For the later members of the series, the evidence for the helical nature of the phase (A*) formed first on cooling the isotropic liquid of either the *R* or the *S* enantiomer (*n*-tridecyloxy to *n*-pentadecyloxy) was obtained by a simple experiment in which the compound was sandwiched between clean glass plates and heated to the isotropic liquid and allowed to cool into the helical A* phase; the phase was found to separate from the liquid in two distinct ways, as shown in Figure 2. In this photomicrograph two textures for the A* phase are shown, one a platelet texture and the other a Grandjean plane texture.[19] The platelet texture in some ways

(19) Grandjean, F. *Compt. Rend.* **1921**, *172*, 71; *Ibid.* **1917**, *166*, 165.

Figure 3. Free-standing film of the smectic A* phase.

resembles the platelet texture of blue phase I, and the Grandjean plane texture appear iridescent and similar in nature to that of the cholesteric phase. As the plane texture nucleates and grows, striations within the texture can be seen. These bands are possibly related to integral multiples of the pitch of the helix of the phase. Subsequent cooling produces a transition to a chiral smectic C* phase, which characteristically exhibits both banded, focal–conic and iridescent, plane textures. The striations on the focal–conic domains in the C* phase, which mirror the positions of the molecular layers, are due to pitch bands and dechiralization lines. Dechiralization lines are produced by defects formed when the helical structure of the bulk of the sample meets the ordered surface layers of the preparation.[20] When cooling through the A* to C* transition, the focal–conic domains of the C* phase grow in the regions of the specimen where the Grandjean texture of the A* phase was previously present. In the Grandjean texture, the axis of the helix of the A* phase is normal to the glass plates, but in the focal–conic domains of the C* phase, it can be seen from the presence of pitch bands and dechiralization lines that the helical axis is approximately parallel to the glass. Therefore, in a situation where the integrity of the layers is maintained through the phase transition, this observation suggests that the helical axes in the A* and C* phases are orthogonal to one another.

Observations of the defects of the A* phase were also made on free-standing films. The texture obtained near the clearing point for the A* phase is shown in Figure 3. In this figure the specimen was heated until it was very close to the isotropic liquid. Some drops of the liquid were detected floating on the surface of the film. The sample was then cooled slowly at a rate of 1° min^{-1}. At the edges of the film where the sample had been liquid, long strands of the A* phase started to grow toward the center of the film, as shown in Figure 3. Such a texture is not normally seen in free-standing films of liquid crystals, and it is inconsistent with the presence of a normal A phase. Cooling of this phase produced a typical plane texture for the chiral smectic C* phase. The pitch of the helix in this phase was found to be comparable to the wavelength of visible light, thereby producing an iridescent texture. In this orientation, the handedness of the helix was determined by the optical rotation and found to be in agreement with the general rules (*R* isomer, right-hand helix; *S* isomer, left-hand helix).[21]

(20) Glogarova, M.; Lejek, L.; Pavel, J.; Janovec, U.; Fousek, F. *Mol. Cryst. Liq. Cryst.* **1983**, *91*, 309.

(21) Goodby, J. W.; Chin, E.; Leslie, T. M.; Geary, J. M.; Patel, J. S. *J. Am. Chem. Soc.* **1986**, *108*, 4729.

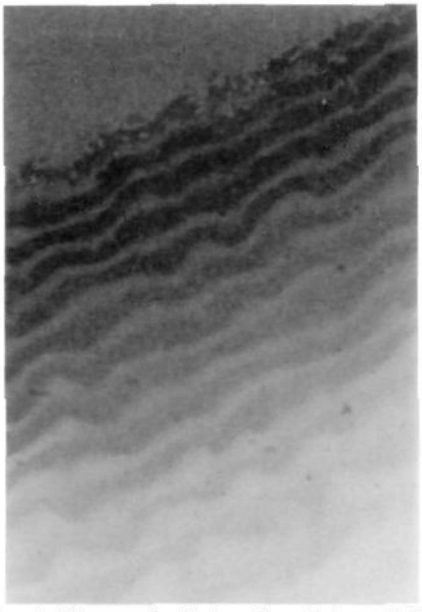

Figure 4. Growth of the smectic A* phase from the isotropic liquid. The material (n = 14) is contained in a cell where the surfaces have been treated with an aligning agent.

Alignment Investigations. In the case of the three propiolates that exhibited the A* phase, epitaxial growth on a homogeneously aligning substrate resulted in the formation of a Grandjean plane texture. The formation of this texture is shown in Figure 4. At the edge of the growing phase, for the liquid to smectic A* transition, parallel lines are observed. These lines are thought to be integral multiples of the pitch of the helix. When the fully developed texture was rotated between crossed polarizers no extinction could be obtained, indicating that the molecules were symetrically disposed to the viewing direction. This property is typical of a helical structure.

In keeping with the orienting properties of the surfactant, cooling into the smectic C* phase produced a focal–conic texture.[22] However, although the molecules were confined within the plane of the cell, a random orientation of the focal–conic domains was obtained. Thus, the aligning agent appears ineffective. This means that there is not preferred direction for the molecules to lie in the plane of the cell. This disordered texture is similar to that obtained when the C* phase is formed directly from the cholesteric phase on cooling.[13]

The application of an electric field to the specimen while it was in its ferroelectric smectic C* phase, at a point near to the C* to A* transition, produced an aligned sample. In the presence of small holding DC voltage (1 V/μm cell thickness), dechiralization lines were observed. These lines were oriented at approximately the tilt angle of the C* phase to the buffing direction and parallel to the molecular layers, indicating that the axis of the helix is in the plane of the cell and perpendicular to the molecular layers. Heating the specimen into the A* phase produced a pattern where the lines were oriented approximately perpendicular to those in the preceding C* phase, thereby giving a texture reminiscent of the cholesteric fingerprint pattern. Thus, this experiment indicates that the helical axis in the A* phase is oriented at approximately right angles to that in the C* phase. The two relevant textures are shown together in Figure 5, where the area of the sample shown is the same in both of the phases. When the holding voltage was removed, the A* phase relaxed back into a Grandjean plane texture with the helical axis normal to the plates of the cell.

Enantiomeric Purity. Racemic modifications of optically active compounds have been used in the past to aid the identification of mesophases in chiral materials. The racemic mixtures of these

(22) Gray, G. W.; Goodby, J. W. *Smectic Liquid Crystals: Textures and Structures*; Leonard-Hill, Glasgow, Scotland, 1984.

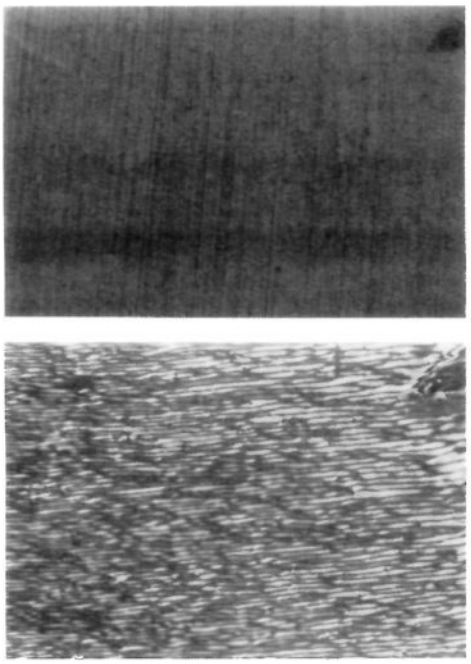

Figure 5. Comparison between the textures (same area) obtained for the C* (upper portion) and A* (lower portion) phases of the (*R*)-tetradecyloxy homologue. The material was confined in a cell constructed of conducting glass. The plate separation was 10 μm. A holding voltage of 5 V DC is being applied to the cell in both cases.

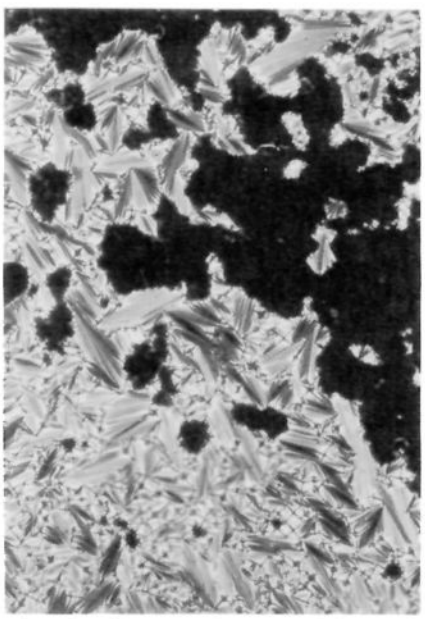

Figure 6. Focal–conic and homeotropic textures of the smectic A phase of the racemic modification of the *n*-tetradecyloxy homologue.

compounds can be obtained either by synthesis from racemic starting materials or by mixing the *R* and *S* enantiomers. The synthetically prepared material was found to exhibit smectic A and smectic C liquid-crystal phases, as shown by Figures 6 and 7. In these photomicrographs, the smectic A phase exhibits typical focal–conic and homeotropic textures, whereas the smectic C phase shows the broken focal–conic and *schileren* patterns.[22]

Alternatively, a racemic mixture can be obtained if the liquids of the *R* and *S* enantiomers are allowed to make a sharp contact between glass plates and then allowed to cool into their liquid-crystalline phases.[3] At the junction of the two materials there is the formation of a racemic modification. Moving away from the contact the proportions of the enantiomers in the mixture change accordingly in order to eventually give either of the pure

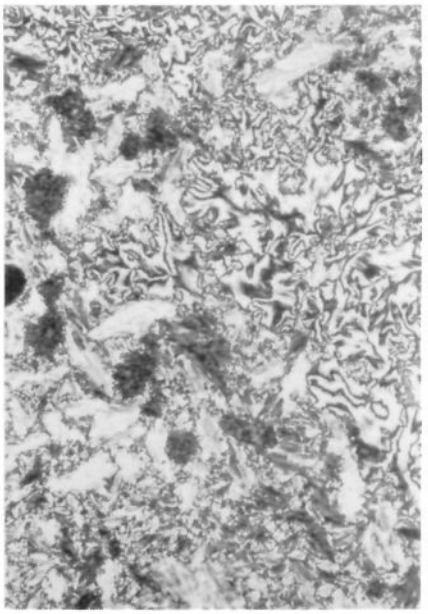

Figure 7. Broken focal–conic and *schlieren* textures of the smectic C phase of the racemic modification of the *n*-tetradecyloxy homologue (same area as in Figure 6).

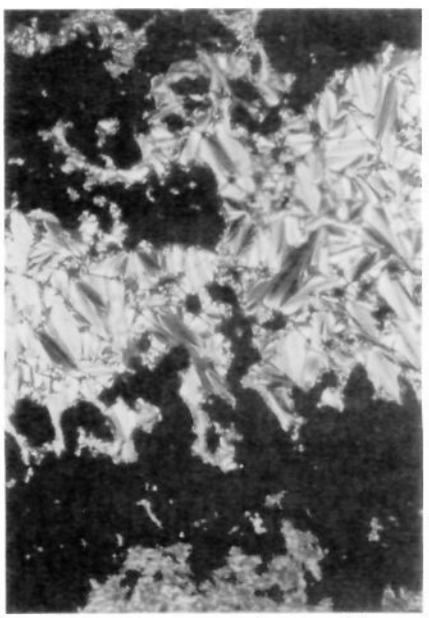

Figure 8. Contact preparation between the *R* and *S* enantiomers of 1-methylheptyl 4′-[[[4″-(*n*-tetradecyloxy)phenyl]propioloyl]oxy]biphenyl-4-carboxylate. The center of the specimen shows the texture of the A phase of the racemic modification, whereas the outer regions of the photomicrograph show the A* textures of the enantiomers.

enantiomers, depending on the direction selected. Thus, a concentration gradient can be observed in the microscope, and the phase changes that occur with varying concentration can be studied as a function of temperature when the sample is placed in an oven. Such an experiment clearly shows that, at the contact, the racemic modification exhibits a smectic A phase, which is recognizable from its focal–conic texture. Moving away from the contact there is a continuous change in texture from a homeotropic to a platelet texture as the A* phase is reached; see Figure 8. As there are no abrupt changes in the texture that might indicate a phase change, this suggests that the A and A* phases are continuously miscible,[23] thereby classifying the helical phase as an A phase. It is also interesting to note that the A phase formed at the contact

(23) Sackmann, H.; Demus, D. *Mol. Cyst. Liq. Cryst.* **1966**, *2*, 81.

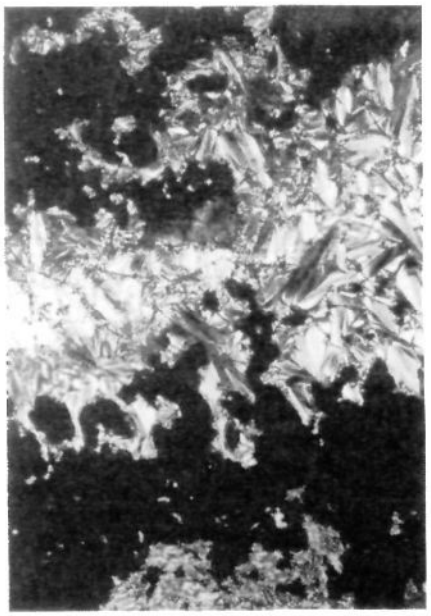

Figure 9. Same area as in Figure 8 except for the materials being in their C and C* phases.

for the racemate appears to be more stable than the A* phase of the enantiomers. Cooling of this preparation results in a transition to the smectic C and C* phases, respectively, as shown in Figure 9.

Thermal Studies. The enthalpies of the transitions were determined by differential scanning calorimetry (DSC). The enthalpy values for the clearing and the melting points of the series are given in Table I. The enthalpy values for the A to C* transitions are not reported because they were generally too small to be measured accurately. This table shows that the enthalpy values for the clearing points fall as the series is ascended. Thus, the first-order clearing point transition apparently becomes increasingly second order in nature as the alkoxy chain is lengthened. However, for the *n*-hexadecyloxy compound, the clearing point enthalpy is much higher than the value for the preceding *n*-tetradecyloxy member. This is due to the fact that the clearing point transition becomes C* to isotropic liquid for the *n*-hexadecyloxy member as the series is ascended, whereas it is still smectic A* to isotropic liquid for the *n*-tetradecyloxy compound.

DSC also shows some distinct differences between the enantiomers and the racemic mixtures for the compounds that have the A* phase. For example, for the *n*-tetradecyloxy homologue, the enthalpies for the A* to isotropic liquid transitions for the enantiomers were found to be at least 4 times smaller than that for the racemic modification. However, the enthalpies for the A to C and A* to C* transitions appear to be approximately equal, as shown in Figure 10. This seems to indicate that the isotropic liquid to mesophase transition becomes weakly first order in nature for either of the enantiomers, whereas it is strongly first order for the analogous racemic modification. Moreover, the differential scanning thermograms for the enantiomers show a broad peak at a temperature where the sample was just above the isotropic liquid transition. This, however, is not the case for the racemic modification. The total enthalpy of the A* to isotropic liquid transition and the broad peak that was seen in the isotropic liquid for any single enantiomer was found to be approximately equal to the enthalpy for the A to isotropic transition for the equivalent racemate. This is clearly shown in Figure 10 for the *n*-tetradecyloxy homologue; the heating cycle for the racemate appears normal, whereas the cooling cycle for the *R* enantiomer has a large diffuse peak just before the transition from the isotropic liquid to the A* phase occurs. This suggests that there are strong pretransitional effects accompanying the transition to and from the A* phase. Although no visible effects were observed by optical microscopy, some diffuse scattering was detected by X-ray diffraction in this temperature range. Apart from pretransitional effects, there is a remote possibility that an extra phase exists in this temperature range, which may be analogous to the blue fog phase in cholesterics (see later). Although this effect is reproducible and reversible for all three of the homologues, it should be remembered that the heating and cooling rates used are not slow enough for the specimens to be considered at true equilibrium. Consequently, the materials have been examined further by adiabatic calorimetry, and the peaks present at the clearing point are still observed under these more rigorous conditions.[24]

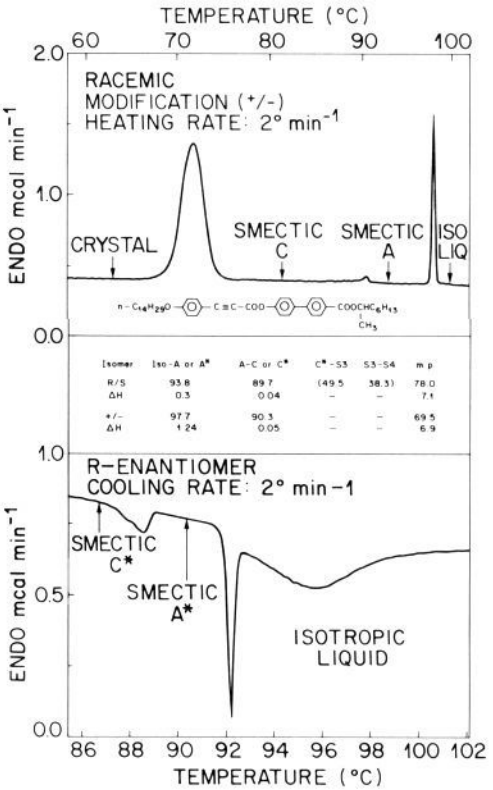

Figure 10. Transition temperatures (°C) and enthalpies of transition (ΔH) for 1-methylheptyl 4′-[[[4″-(*n*-tetradecyloxy)phenyl]propioloyl]-oxy]biphenyl-4-carboxylate. The upper thermogram shows the melting process for the racemic modification, whereas the lower trace shows the cooling process for the *R* enantiomer. The heating and cooling rates were 2° min^{-1}.

Structural Studies. The principal X-ray study consisted of 2θ scans through the smectic layer peak. The temperature dependence of the peak position (layer spacing) for the three enantiomers is shown in Figure 11. It can be seen that, upon heating, the peak position for each of the enantiomers continuously increases and, for the *n*-dodecyloxy and *n*-tetradecyloxy homologues, saturates in the smectic A* phase at a nearly constant value. The value of the smectic A* layer spacing was found to be commensurate with the fully extended molecular length of the molecule. Assuming that the ratio of the smectic C* to smectic A* layer spacing is proportional to the cosine of the smectic C* tilt angle, at the lowest measured temperature for the *n*-dodecyloxy homologue the layer spacing ratio was found to yield a smectic C* tilt angle of 24.4°. For the *n*-hexadecyloxy member the layer spacing increases continuously as the sample is heated, until the transition to the isotropic liquid is reached. The X-ray scans indicate that the A* phase does not occur for this compound. This result is consistent with optical and thermal data.

Two other important features of the X-ray data are shown in the inset of Figure 11, which contains layer peak scans taken within the smectic C*, smectic A*, and isotropic phases of the (*R*)-*n*-tetradecyloxy enantiomer. First, it is evident that, within in-

(24) Huang, C. C., personal communication.

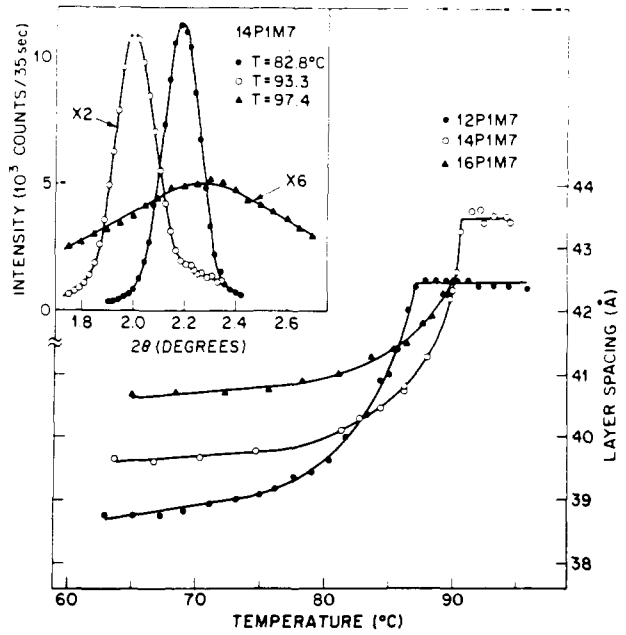

Figure 11. Temperature dependence of the layer spacing for the n = 12, 14, and 16 R enantiomers. The inset shows scans through the layer peak for the n = 14 enantiomers at temperatures within the smectic C* (closed circles), smectic A* (open circles), and just into the isotropic phase (triangles).

strumental resolution, the layer peak widths in the smectic C* and smectic A* phases are comparable, and the integrated intensity in these peaks only differs by a factor of 2. This implies that the smectic A* layer correlations extend a minimum distance of 10 layers, thereby establishing smectic layering as a key structural element of the smectic A* phase. Second, at a temperature just above the smectic A* to isotropic liquid transition, a diffuse layer peak is seen with a peak position comparable to a layer peak position measured well within the temperature range of the smectic C* phase. One possible explanation for this observation is that small smectic C* regions are present within the isotropic phase. These may result from fluctuations of the low-temperature phase or they are an intrinsic feature of an intermediate phase. This latter possibility will be discussed in the concluding section of this article.

Spontaneous Polarization Studies. The spontaneous polarization in the smectic C* phases of the n-dodecyl, n-tetradecyl, and n-hexadecyloxy members of the series was measured as a function of temperature, as described previously.[14] The results are shown for the three compounds in Figure 12. All three show relatively large polarizations in the region of 100 nC cm^{-2}, with the maximum value descending as the series is ascended. This is to be expected, as the density of dipoles falls as the molecular dimensions increase when the series is ascended. The direction of the spontaneous polarization for the three was determined and found to fall into the postulated pattern described previously.[21] (R isomer, Ps(−); S isomer, Ps(+). At the transition from the C* phase to the A* phase some unusual effects were observed; however, these will not be discussed here but will be reported on in detail subsequently.[25]

For all three of the materials studied, at temperatures 30–40° below the Curie point, abnormalities were seen in the polarization data. These abnormalities were usually detected by a fall in the value of the polarization (see Figure 12), and by changes in the switching behavior of the sample. However, at much higher field strengths (~80 V/μm), above the saturation limit, the measured polarization was found to be approximately equal to the expected value. Furthermore, the point at which the fall in the value of the polarization was detected for each material was found to

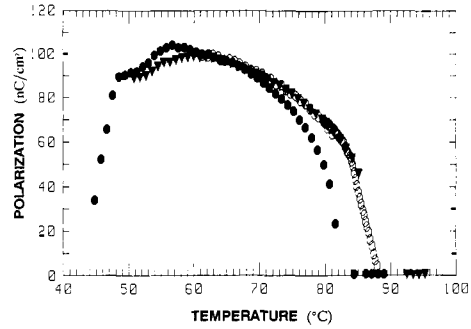

Figure 12. Spontaneous polarization (nC cm^{-2}) measured as a function of temperature for the n-dodecyl n = 12, ●), n-tetradecyl (n = 14, ○), and n-hexadecyl (n = 16, ▼), homologues.

correspond roughly to the temperature of a smectic C* to S3 transition. This suggests that there is a link between the apparent phase transitions and the behavior of the polarization.

Discussion

The facts from these experiments show that the phase formed on cooling the isotropic liquid of the n-tridecyl to n-pentadecyl enantiomers has a layered structure of the smectic A type. Optical studies show that the new phase is similar in nature to the cholesteric phase and therefore has a helical structure. The direction of the helix was shown to be orthogonal to that in the smectic C* phase. In aligned cells the direction of the helix in the A* phase was shown to be parallel to the layers. Thus, we have a newly defined phase that has properties of both cholesteric and smectic A mesophase. Moreover, this phase appears in the homologous series at a point where the smectic A temperature range is becoming shorter. In the case of all three of the optically active homologues described, this range is only a few degrees. It is to be expected, as this range is so short, that the molecular fluctuations will be quite extensive and will be influenced by pretransitional effects from both the smectic C* phase and the isotropic liquid. This will lead to a fairly disordered smectic A phase where the layers are not particularly well-defined. In the presence of a high degree of molecular chirality such a structure might then be able to support the presence of a helix, whereas a structure that has relatively well-defined layers, i.e., with fewer fluctuations, would probably not be able to form such a twisted structure.

The qualitative model that emerges for the structure of this phase is one where the elongated molecules are arranged in loosely ordered layers with their long axes either normal or only slightly tilted with respect to the layer planes. In the direction of the layer planes there is a twist in the parallel orientation of the molecules. This twist can be effected by either having defects, such as screw dislocations, between short sections of the A phase or by having some cholesteric liquidlike regions separating larger smectic A domains, as shown in Figure 1. The full details of the structure of this novel state are currently being elucidated by high-resolution X-ray diffraction on aligned samples and by freeze fracture studies. The results obtained from these investigations will be reported shortly.

Earlier de Gennes predicted[26] that, just as magnetic flux can penetrate type II superconductors in a lattice of vortexes, twist or bend distortions can be incorporated into a layered smectic A structure by the presence of an array of screw or edge dislocations. De Gennes demonstrated for a nematic–smectic A material that this possibility would occur at a point where the nematic to smectic A transition became second order and when the A phase would have large molecular fluctuations.

A model for such an array of dislocations was recently proposed for the cholesteric to smectic A transition by Renn and Lubensky.[27] With reference to the structure of the A* phase shown in Figure 1, their model specifies that grain boundaries of screw dislocations are responsible for rotating the individual "blocks" of the smectic

(25) Sin-Doo Lee; Patel, J. S.; Goodby, J. W.; Waugh, M. A. Submitted to *Phys. Lett.*

(26) de Gennes, P. G. *Solid State Commun.* **1972**, *10*, 753.
(27) Renn, S. R.; Lubensky, T. C. Submitted to *Phys. Rev. A.*

A* layers with respect to each other. The resultant phase is referred to as a twist grain boundary (TGB) phase. They predicted this phase can occur between the cholesteric and the smectic A phase in a way similar to how the Abrikosov flux lattice phase can occur between the normal and the superconducting phases.[28] Renn and Lubensky further established that the requirement for this intermediate phase to occur is that the Ginzburg parameter, which is equal to the ratio of the twist penetration length (λ_T) to the smectic A correlation length (ξ), must ge greater than $1/2^{1/2}$.

Thus, the TGB phase could be a feasible model for the smectic A* phase, for the following reasons. First, the X-ray scattering predicted for the TGB phase is consistent with our X-ray measurements on the A* phase. Second, the model predicts a helical structure with a helical axis parallel to the smectic layers, which is consistent with our optical experiments. Last, we observe the A* phase in the vicinity of a smectic A to smectic C* transition where the A phase has a short temperature range. At such a transition, λ_T diverges, which results in a large value for the Ginzburg parameter, as required by the theory.[29] Hence, the TGB phase is a viable model for the A* phase. As a consequence, we can explore the implications of this possibility still further, and in particular, we can speculate on the nature of the effect observed between the A* phase and the isotropic phase. For the superconducting flux lattice it has been proposed,[30] and observed,[31] that the vortex lattice can disorder into an entangled or disentangled fluid of vortexes. We suggest that a similar disordering of the regular array of screw dislocations in the TGB phase may be the mechanism responsible for the occurrence of the phase observed in the isotropic liquid just above the A* phase.

Finally, we should make some comments on the use of the notation A* to describe the new phase. Without the presence of optically active material the smectic A phase is a nonchiral phase. However, if the phase contains chiral molecules the phase can become chiral. This can be achieved by perturbing the structure of the phase in an applied field or by distorting the structure mechanically. In both of these situations the symmetry of the phase is broken, resulting in electroclinic or flexoelectric behavior. In the new phase the symmetry is also broken by the helical structure, but in this case it is not achieved by external forces. Therefore, the phase can be appropriately designated A*. However, the complications involving space symmetry and helicity in these mesophases show that the nomenclature system is in need of serious review.

(28) Abrikosov, A. A. *Sov. Phys.—JETP (Engl. Transl.)* **1957**, *5*, 1174.
(29) Meyer, R. B., personal communication.
(30) Nelson, D. R. *Phys. Rev. Lett.* **1988**, *60*, 1973.
(31) Gammel, P. L.; Bishop, D. J.; Dolan, G. J.; Kwo, J. R.; Murray, C. A.; Schneemeyer, L. F.; Waszaczak, J. *Phys. Rev. Lett.* **1987**, *59*, 2592.

Summary

We have discovered a new helical liquid crystal and have shown that it is analogous to a twisted smectic A phase. Therefore we have classified the phase as smectic A*. The helix was found to propagate in a direction parallel to the layers, thereby producing twist distortions within the layers. It is suggested that these distortions are possibly organized into a lattice of screw dislocations.

Acknowledgment. We thank Professors T. Lubensky and R. Meyer for stimulating discussions.

Registry No. (*R*)-$C_8H_{17}O$-*p*-C_6H_4-C≡CCOO-*p*-C_6H_4-*p*-C_6H_4-$COOCH(CH_3)C_6H_{13}$, 122521-57-7; (*S*)-$C_8H_{17}O$-*p*-C_6H_4-C≡CCOO-*p*-C_6H_4-*p*-C_6H_4-$COOCH(CH_3)C_6H_{13}$, 122521-61-3; (*R*)-$C_9H_{19}O$-*p*-C_6H_4-C≡CCOO-*p*-C_6H_4-*p*-C_6H_4-$COOCH(CH_3)C_6H_{13}$, 122521-58-8; (*S*)-$C_9H_{19}O$-*p*-C_6H_4-C≡CCOO-*p*-C_6H_4-*p*-C_6H_4-*p*-C_6H_4-$COOCH(CH_3)C_6H_{13}$, 122521-62-4; (*R*)-$C_{10}H_{21}O$-*p*-C_6H_4-C≡CCOO-*p*-C_6H_4-*p*-C_6H_4-$COOCH(CH_3)C_6H_{13}$, 122521-59-9; (*S*)-$C_{10}H_{21}O$-*p*-C_6H_4-C≡CCOO-*p*-C_6H_4-*p*-C_6H_4-$COOCH(CH_3)C_6H_{13}$, 122521-63-5; (*R*)-$C_{11}H_{23}O$-*p*-C_6H_4-C≡CCOO-*p*-C_6H_4-*p*-C_6H_4-$COOCH(CH_3)C_6H_{13}$, 122521-60-2; (*S*)-$C_{11}H_{23}O$-*p*-C_6H_4-C≡CCOO-*p*-C_6H_4-*p*-C_6H_4-$COOCH(CH_3)C_6H_{13}$, 122521-64-6; (*R*)-$C_{12}H_{25}O$-*p*-C_6H_4-C≡CCOO-*p*-C_6H_4-*p*-C_6H_4-$COOCH(CH_3)C_6H_{13}$, 120551-07-7; (*S*)-$C_{12}H_{25}O$-*p*-C_6H_4-C≡CCOO-*p*-C_6H_4-*p*-C_6H_4-$COOCH(CH_3)C_6H_{13}$, 122521-65-7; (*R*)-$C_{13}H_{27}O$-*p*-C_6H_4-C≡CCOO-*p*-C_6H_4-*p*-C_6H_4-$COOCH(CH_3)C_6H_{13}$, 120551-01-1; (*S*)-$C_{13}H_{27}O$-*p*-C_6H_4-C≡CCOO-*p*-C_6H_4-*p*-C_6H_4-$COOCH(CH_3)C_6H_{13}$, 120551-04-4; (*R*)-$C_{14}H_{29}O$-*p*-C_6H_4-C≡CCOO-*p*-C_6H_4-*p*-C_6H_4-$COOCH(CH_3)C_6H_{13}$, 120551-02-2; (*S*)-$C_{14}H_{29}O$-*p*-C_6H_4-C≡CCOO-*p*-C_6H_4-*p*-C_6H_4-$COOCH(CH_3)C_6H_{13}$, 120551-05-5; (*R*)-$C_{15}H_{31}O$-*p*-C_6H_4-C≡CCOO-*p*-C_6H_4-*p*-C_6H_4-$COOCH(CH_3)C_6H_{13}$, 120551-03-3; (*S*)-$C_{15}H_{31}O$-*p*-C_6H_4-C≡CCOO-*p*-C_6H_4-*p*-C_6H_4-$COOCH(CH_3)C_6H_{13}$, 120551-06-6; (*R*)-$C_{16}H_{33}O$-*p*-C_6H_4-C≡CCOO-*p*-C_6H_4-*p*-C_6H_4-$COOCH(CH_3)C_6H_{13}$, 120551-08-8; (*S*)-$C_{16}H_{33}O$-*p*-C_6H_4-C≡CCOO-*p*-C_6H_4-*p*-C_6H_4-$COOCH(CH_3)C_6H_{13}$, 122521-66-8.

Palladium Carbonyl Clusters Entrapped in NaY Zeolite Cages: Ligand Dissociation and Cluster–Wall Interactions

Lien-Lung Sheu, Helmut Knözinger,† and Wolfgang M. H. Sachtler*,‡

Contribution from the V.N. Ipatieff Laboratory, Center for Catalysis and Surface Science, Northwestern University, Evanston, Illinois 60208. *Received April 13, 1989*

Abstract: Highly structured FTIR spectra, which are indicative of Pd carbonyl clusters, are obtained after adsorption of CO on Pd/NaY which was reduced at 200 °C, but broad IR bands are observed with samples which were reduced at higher temperatures. Pd carbonyl clusters with only CO ligands have not been reported previously, which indicates that the geometry of NaY supercages favors their formation. As the clusters lose some of their CO ligands, old IR bands erode and new IR bands with sharp isosbestic points emerge. This process is entirely reversed upon reintroduction of CO. The low activation energy of CO release and concomitant changes in the IR band characteristic of zeolite O–H vibrations indicate a chemical interaction of zeolite protons and Pd carbonyl clusters.

Zeolite-supported, highly dispersed metal catalysts have steadily gained importance since the pioneering work by Rabo et al.[1] The combination of the catalytic properties of transition metals with the steric constraints imposed by the zeolite structure carries great potential for active and selective catalysts. A combination of

† Institut für physikalische Chemie der Universität München, West Germany
‡ Present address: Technical Center, The BOC Group, Inc., 100 Mountain Avenue, Murray Hill, New Jersey 07974.

(1) Rabo, J. A.; Pickert, P. E.; Mays, R. L. *Ind. Eng. Chem.* **1961**, *53*, 733.

0002-7863/89/1511-8125$01.50/0